Analysis Effect of Modifications Motorcycle Swing Arm on Mechanical Characteristics Using Finite Element Method

***Faturohman Yuniarto*[1,2]*,Ismi Choirotin*[1*]*, Lee Tsai-Cheng*[2]**

[1]Mechanical Engineering Study Program, Faculty of Engineering, Universitas Islam Malang, Malang, Indonesia
[2]Department of Mechanical and Vehicle Engineering, Faculty Engineering, St. John's University, New Taipei City, Taiwan
e-mail :22201052069@unisma.ac.id
*ismi.choirotin@unisma.ac.id

ABSTRACT

Reducing the mass of a motorcycle swing arm through perforated structures is a common lightweight design strategy, but introducing perforations may alter the stress distribution and reduce structural safety. This study analyzes the mechanical characteristics of a solid swing arm and two perforated swing arm configurations, Model A and Model B, made of Aluminum 6061-T6 under a static load of 1000 N using three-dimensional finite element simulation. Equivalent stress, total deformation, factor of safety, and structural mass were compared among the three models after the numerical model was verified through a mesh independence study. The results show that perforation increases the maximum equivalent stress and total deformation while reducing the factor of safety and structural mass relative to the solid model. Nevertheless, the maximum stress in every configuration remained well below the material yield strength, confirming that all three designs remain structurally safe under the applied load.

Keywords: *swing arm; perforated structure; finite element method; von Mises stress; total deformation; factor of safety; Aluminum 6061-T6*

INTRODUCTION

Advances in automotive technology continue to drive the development of lighter vehicle components to improve motorcycle efficiency and performance. Reducing structural mass lowers the vehicle's workload, improves fuel efficiency, and enhances handling and acceleration, making lightweight design an important factor in the transition toward low-emission and energy-efficient transportation [1]. The swing arm is a primary component of the rear suspension system that connects the vehicle frame to the rear wheel and transmits the static and dynamic loads generated by the vehicle weight, acceleration, braking, and cornering forces. Because the swing arm experiences repeated loading during operation, geometric modifications such as the introduction of holes or local material removal can significantly influence its stress distribution and deformation behavior, so numerical simulation is required to evaluate these effects before a modified design is applied in practice [2].

Perforated swing arm designs are common among aftermarket motorcycle components because holes reduce structural mass without changing the overall shape of the part, although they may also alter the distribution of internal stress and therefore require structural evaluation. Several previous studies support this trade-off. A generative-design optimization of a swing arm using aluminum alloys achieved a mass reduction of 34.32–36.91% while keeping the equivalent stress, deformation, and safety factor within acceptable limits, with Al 6061-T6 providing the best combination of stress and safety performance among the materials tested [3]. A lightweight single-sided swing arm produced through generative design in Al 6061 similarly reached a maximum equivalent stress of 99.1 MPa and a safety factor of 2.77, with a lower mass than an equivalent Al 7075 design [4]. Investigations of perforated aluminum members have further shown that increasing the hole-diameter ratio can reduce buckling resistance by up to 9.7%, while the stress concentration factor around a circular hole in a loaded plate can exceed 2.6 depending on the hole-to-width ratio, confirming that perforations reliably raise local stress even as they reduce mass [5, 6]. A comparison of swing arm materials modeled in CATIA and analyzed in ANSYS also found that material selection strongly affects stiffness and strength [7], reinforcing the need for a systematic structural comparison whenever the geometry of a swing arm is modified.

Although these studies demonstrate that lightweight redesign can reduce swing arm mass without necessarily compromising safety, direct structural comparisons between a solid swing arm and multiple perforated hole configurations of the same base geometry remain limited. This study therefore evaluates the effect of two perforated swing arm configurations, Model A and Model B, on the equivalent stress distribution, total deformation, and factor of safety relative to a solid swing arm and examines whether the resulting designs still satisfy the structural safety criteria under a representative static load. The results are intended to provide a reference for evaluating aftermarket swing arm modifications while maintaining structural safety and reliability.

RESEARCH METHOD

General Approach

This study used a quantitative, comparative research design based on three-dimensional finite element simulations performed in SolidWorks Simulation. The finite element method (FEM) discretizes a continuous structure into a finite number of interconnected elements so that a complex geometry can be analyzed through a system of algebraic equations relation nodal forces and displacements [8]. Three swing arm models with an identical overall length of 48 cm were compared: a solid swing arm and two perforated configurations, Model A and Model B, which differ from the solid design only in the size, number, and location of the perforations, without altering the primary dimensions of the part. All models were assigned Aluminum 6061-T6 as a homogeneous, isotropic, linear elastic material, with the properties summarized in Table 1.

Table 1. Material specification of Aluminum 6061-T6

Property	Value
Density (ρ)	2700 kg/m³
Modulus of elasticity (E)	69 GPa
Poisson's ratio (ν)	0.33
Yield stress (σy)	275 MPa
Ultimate stress (σu)	310 MPa
Fatigue limit (σf)	96 MPa

Boundary Conditions and Loading

A static load of 1000 N was applied at the shock-absorber mounting point, oriented perpendicular to the mounting surface and directed downward to represent the force transmitted through the rear suspension by the combined weight of the motorcycle and rider. Both pivot holes, which represent the connection between the swing arm and the motorcycle frame, were fully fixed, restricting all translational and rotational degrees of freedom (Fig. 1), so that the resulting equivalent (von Mises) stress, total deformation, and factor of safety reflect the response to the applied load alone.

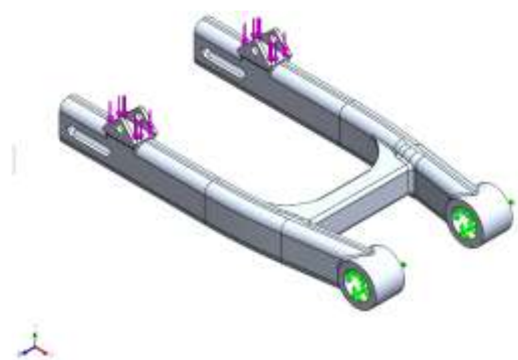

Figure 1. Fixed pivot supports and applied load at the shock-absorber mount.

Mesh Independence and Model Validation

A mesh independence study was performed by refining the global mesh size from 4.0 mm to 3.1 mm and recording the resulting maximum equivalent stress at each step. Because the variation between successive refinements remained below the 1% convergence criterion throughout this range (0.05–0.65%), the 3.1 mm mesh (Fig. 2) was adopted for all subsequent simulations, providing the finest discretization among the converged mesh sizes. The finite element model was further checked against an analytical beam-deflection calculation for the solid swing arm, idealized as a simple cantilever beam with span L = 353 mm and section moment of inertia I_y = 254,019.73 mm⁴ obtained from the CAD model, using the standard deflection relation:

$$\delta = PL^3 / 3EI \tag{1}$$

This analytical model predicted a deflection of 0.418 mm, compared with 0.391 mm from the finite element simulation, a difference of 0.069%. The discrepancy is attributed to the simplified cross-section, geometry, and boundary conditions of the analytical beam model, whereas the three-dimensional finite element model captures the actual swing arm geometry, local stress concentrations, and true boundary conditions; the analytical result nonetheless confirms that the finite element model reproduces the correct order of magnitude and overall structural trend.

Figure 2. Finite element mesh of the swing arm at the adopted 3.1 mm element size.

Data Processing

For each model, the simulation results were compared in terms of equivalent (von Mises) stress, total deformation, factor of safety, and structural mass. The percentage change in stress and deformation of each perforated model (subscript p) relative to the solid model (subscript s) was calculated as

$$\%\Delta\sigma = [(\sigma_p - \sigma_s) / \sigma_s] \times 100\% \qquad (2)$$

$$\%\Delta\delta = [(\delta_p - \delta_s) / \delta_s] \times 100\% \qquad (3)$$

RESULTS AND DISCUSSION

Equivalent Stress Distribution

The maximum equivalent (von Mises) stress obtained from the finite element simulation was 21.291 MPa for the solid swing arm, 24.922 MPa for Model A, and 26.285 MPa for Model B (Fig. 3), corresponding to increases of 17.05% and 23.46%, respectively, relative to the solid model. In every model, the highest stress occurred at a geometric discontinuity: at the junction between the swing arm and the pivot housing in the solid model, and around the edges of the perforations nearest the shock-absorber mount in the perforated models (Fig. 4), where the reduced cross-sectional area concentrates the load transferred from the shock-absorber mount toward the pivot region. In the perforated models, the pivot region itself remained close to the stress level of the solid model, around 21–22 MPa, indicating that once holes are introduced, the perforations rather than the pivot connection govern the critical stress location.

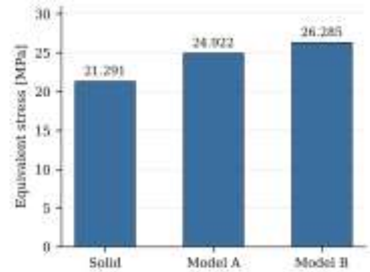

Figure 3. Maximum equivalent stress by swing arm model.

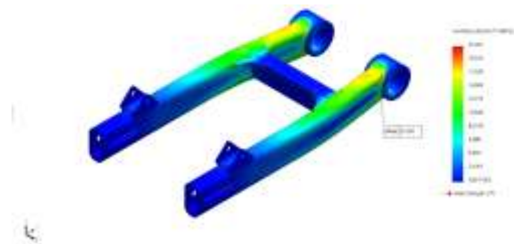

(a) Solid Swing Arm

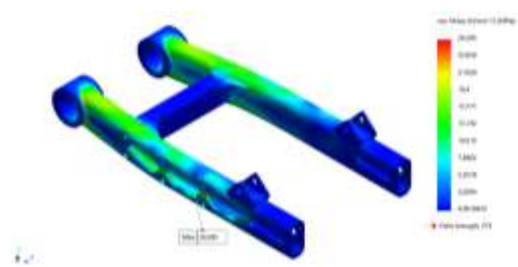

(b) Perforated Swing Arm Model B

Figure 4. Equivalent (von Mises) stress distribution: (a) solid swing arm; (b) perforated swing arm Model B.

Total Deformation and Stiffness

The total deformation followed the same trend as the equivalent stress. The solid swing arm exhibited the smallest total deformation, 0.555 mm, while Model A and Model B exhibited 0.621 mm and 0.603 mm, respectively (Fig. 5), corresponding to increases of 11.89% and 8.65% relative to the solid model. In all three models, the maximum deformation occurred at the loading point at the end of the swing arm, while the minimum deformation occurred at the fixed pivot region, consistent with the expected response of a cantilever-like structure. Because the perforations reduce the effective cross-sectional area and second moment of area, they lower the bending stiffness of the structure; Model A, which shows the largest total deformation among the three designs, experiences the greatest loss of stiffness, whereas Model B better preserves the overall stiffness despite carrying the higher local stress described above.

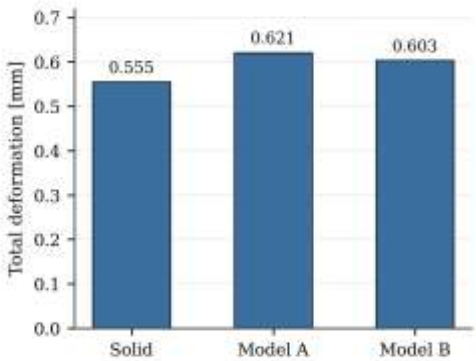

Figure 5. Total deformation by swing arm model.

Factors of Safety, Mass, and Overall Comparison

Table 2 summarizes the equivalent stress, total deformation, factor of safety, and mass obtained for the three models. The factor of safety decreased from 12.541 for the solid swing arm to 10.713 for Model A and 10.158 for Model B, the lowest value among the three configurations, while the structural mass decreased from 2232.63 g for the solid model to 2066.46 g for Model A, a reduction of 166.17 g (7.44%), and to 2082.39 g for Model B, a reduction of 150.24 g (6.73%). These results show that Model A achieves the greatest mass reduction but the largest loss of stiffness, whereas Model B offers a comparatively more balanced trade-off between mass reduction and stiffness at the cost of the highest localized stress concentration. Despite these differences, the maximum equivalent stress of all three models remains well below the yield strength of Aluminum 6061-T6, 275 MPa, so every configuration operates within the elastic range and satisfies the structural safety criteria, with a factor of safety greater than 1, under the applied static load of 1000 N.

Table 2. Recap of simulation results for the three swing arm models

Model	σmax [MPa]	δ [mm]	FOS	Mass [g]
Solid	21.291	0.555	12.541	2232.63
Model A	24.922	0.621	10.713	2066.46
Model B	26.285	0.603	10.158	2082.39

CONCLUSION

Finite element simulation of a solid swing arm and two perforated swing arm configurations under a static load of 1000 N shows that introducing perforations increases the maximum equivalent stress and total deformation while reducing the factor of safety and structural mass compared with the solid design. The solid swing arm provided the best overall structural performance, with the lowest equivalent stress, 21.291 MPa, the smallest total deformation, 0.555 mm, and the highest factor of safety, 12.541, whereas Model A achieved the greatest mass reduction, 7.44%, at the cost of the largest increase in deformation, and Model B offered a more balanced compromise between weight reduction and stiffness despite exhibiting the highest local stress concentration. In all three configurations, the maximum equivalent stress remained well below the yield strength of Aluminum 6061-T6, confirming that every design remains within the elastic range and satisfies the structural safety criteria under the evaluated loading condition. These findings indicate that perforation is a feasible strategy for lightweight swing arm design, provided that the hole geometry and arrangement are optimized to balance mass reduction against stiffness and stress concentration. Future work should validate these numerical results experimentally and extend the analysis to dynamic and fatigue loading, welded-joint and contact interactions, and environmental effects such as temperature, corrosion, and vibration.

NOMENCLATURE

σ	equivalent (von Mises) stress	[MPa]
ε	normal strain	[–]
E	modulus of elasticity	[GPa]
P	applied load	[N]
A	cross-sectional area	[mm²]
L	length / span	[mm]
I	second moment of area	[mm⁴]

Greek letters

δ	deformation / displacement	[mm]
v	Poisson's ratio	[–]

Subscripts

p	perforated model
s	solid model

REFERENCES

1. Vemunuri, A. C., Quantifying the Weight Reductions of Vehicle Body Structures through Material Substitution and the Impact of Lightweight on Fuel Efficiency and Harmful Gas Emissions, Purdue University, 2025.
2. Spanoudakis, P., Christenas, E., Tsourveloudis, N. C., Design and Structural Analysis of a Front Single-Sided Swingarm for an Electric Three-

Wheel Motorcycle, Applied Sciences (Switzerland), Vol. 10, No. 17, 2020.

3. Gupta, G. S., Prithvi, C. H., Chowdary, S. J., Design and Analysis of Light Weight Swing Arm Using Generative Design Concept, E3S Web of Conferences, Vol. 552, 2024.
4. Balasubramanian, A., Shaktivel, G., Raghukiran, N., Light-Weighting of Single-Sided Motorcycle Swing-Arm through Generative Design, IOP Conference Series: Materials Science and Engineering, Vol. 1128, No. 1, 2021.
5. Sun, X., Fu, J., Sun, G., Effect of Web Perforations on the Web Buckling Resistance of 7075-T6 and AA-6086 High-Strength Aluminium Alloy C-Shaped Members under End-Two-Flange Loading Case, Buildings, Vol. 13, No. 8, 2023.
6. Zengah, S., Baltach, A., Djebli, A., Benhamena, A., Compilation of Stress Concentration Factors in the Vicinity of a Geometric Discontinuity in Structures, Acta Universitatis Sapientiae, Electrical and Mechanical Engineering, Vol. 16, pp 1-15, 2024.
7. Mahith, J., Balaji, G., Jeevan Kumaar, N., Design and Analysis of Swing Arm, Tuijin Jishu/Journal of Propulsion Technology, Vol. 45, No. 3, 2024.
8. Chandrupatla, T. R., Belegundu, A. D., Introduction to Finite Elements in Engineering, Pearson, 2012.